Dielectric and vibrational properties of bixbyite sesquioxides

Pietro Delugas,[1,2] Vincenzo Fiorentini,[2,3] and Alessio Filippetti[2]
[1]*CNR-IMM, Stradale Primosole, 95121 Catania, Italy*
[2]*CNR-INFM-SLACS, Cittadella Universitaria, Monserrato, 09042 Cagliari, Italy*
[3]*Dipartimento di Fisica, Università di Cagliari, Cittadella Universitaria, Monserrato, 09042 Cagliari, Italy*
(Received 9 July 2009; revised manuscript received 21 August 2009; published 18 September 2009; corrected 16 October 2009)

Most sesquioxides (X_2O_3) with a rare-earth cation crystallize in the cubic structure known as bixbyite, also adopted by oxides with smaller trivalent cations (e.g., Sc and Y). Here we discuss the dielectric behavior of these crystals on the basis of results of density-functional calculations for a selection of them, namely, Sc, La, Dy, and Lu binary sesquioxides. Vibrational modes can be categorized in two groups: one mostly localized on cations and with low frequencies and another with higher energies localized on oxygens. In rare-earth oxides the frequency of cation-localized modes shows a weak dependence on cation type; oxygen modes, instead, increase their energy as the cation radius decreases from La to Lu. In the case of the smaller Sc, frequencies increase for all modes and the smaller cation/oxygen mass ratio allows for a significant mixing of oxygen and cation displacements at intermediate frequencies. In the final analysis, we conclude that bixbyites all have relatively small dielectric constants and rationalize the reasons thereof.

DOI: 10.1103/PhysRevB.80.104301 PACS number(s): 77.84.Bw, 63.20.−e, 78.30.−j

I. INTRODUCTION

The evolution of complementary metal-oxide-semiconductor technology is causing the gradual replacement of the native Si oxide as the insulating layer of metal-oxide-semiconductor junctions by thicker layer of more responsive dielectric media.[1,2] This improves both the electrical leakage reliability and the capacitive density of the junctions. The materials in question have large electronic gap (5 eV, say) and a large dielectric constant ε (say, upward of 20–25). Due to the large gap, their high-frequency electronic screening is modest and the electronic contribution ε_∞ is small (of order 3–5); the enhanced total ε must therefore come from lattice response (which is in fact very small in the native silicon oxide). Among possible high-ε materials, rare-earths oxides have been quite popular.[3] Not only are they good insulators with large band gaps and appreciable lattice dielectric screening; they are also expected to be stable in contact with Si and to form morphologically clean interfaces.[4,5] The studies on rare-earth oxides involved either the binary R_2O_3 sesquioxides they form by themselves, or the many complex oxides, mostly RBO_3 perovskitic oxides, which involve other smaller cations occupying the B site while the rare-earths cations are placed at the R site. Some of these smaller trivalent cations, such as Sc or Y, in fact form sesquioxides with the same crystal structure as rare earths. Because of their similar properties, Sc and Y oxides are often considered together with rare-earths ones.

Complex oxides have usually better dielectric constants than most part of the sesquioxides. Perovskites have dielectric constants ordinarily well above 20,[6] whereas byxbyite sesquioxides are generally in the 12–20 range. (Hexagonal La_2O_3 and Pr_2O_3 reach values[7] of 25 but their cubic phases are in line with the others.) Our previous study[8] of bixbyite Lu_2O_3 showed that only oxygen displacements are able to produce large dipoles, whereas cation displacements have dipoles at least an order of magnitude lower. The modes involving oxygen displacements are placed at higher frequencies with respect to modes involving cation displacements. High frequencies reduce [see Eq. (5) below] screening by large-dipole modes. Does this picture apply to all bixbyites? Plausibly, yes, since the distinction between low-dipole cation displacements at low frequency and oxygen large-dipole displacements at higher frequency should hold whenever the cation/oxygen mass ratio is large enough. Also, the ineffectiveness in inducing dipoles should be a common feature to all cations arranged in the bixbyite structure.

In this paper we give a quantitative assessment of the above considerations. We present first-principles computations of zone-center vibrational modes, effective dynamical charges, and dielectric constants for bixbyites with different cations: Sc, La, and Dy. These cations (together with our previously studied[8] Lu) span the whole size and mass range for cations in bixbyites. Sc is significantly less massive than the others (only three times heavier than oxygen) and its bonds with oxygen are stiffer than for rare earths. The ionic radius of La is large and the La_2O_3 cubic phase is actually disfavored with respect to the hexagonal one. Dy_2O_3 is expected to behave as a typical bixbyite rare-earth cation with intermediate properties between La and Lu.

II. METHOD

The lattice contributes to the dielectric constant of a crystal when periodic ionic displacements induce finite dipole densities[9,10] and then only if the crystal fulfills certain symmetry requirements. The induced dipole is linear in the displacements (for small displacements). The dipole density corresponding to a generic displacement can be calculated once the induced dipole for a complete displacement basis set is known. Choosing as a basis the (periodic) shifts of each ion along the cartesian directions, the derivatives of macroscopic polarization with respect to such displacements can be viewed as generalized charges of the ions involved. These are usually called[11,12] Born dynamical charge tensors

$$Z^{\star}_{\kappa,\alpha\beta} = \Omega \cdot \frac{\partial P^{\alpha}}{\partial \tau_{\kappa,\beta}}, \tag{1}$$

where $\mathbf{P}$ is the macroscopic polarization and $\boldsymbol{\tau}_{\kappa}$ are the ionic coordinates of the κth atom (α, etc. are cartesian indexes and Ω the crystal volume). For a generic periodic displacement $\mathbf{u}$ we have thus that the induced dipole per unit cell is

$$Z_{\alpha} = \sum_{\kappa\beta} u_{\kappa\beta} Z^{\star}_{\kappa,\alpha\beta}. \tag{2}$$

To calculate the lattice part of the dielectric constant, one chooses as a basis set for lattice periodic displacements the generalized eigenmodes of the zone-center ($\mathbf{k}=0$) dynamical matrix

$$\sum_{\kappa'\beta} \frac{\partial^2 V}{\partial \tau_{\kappa\alpha}\, \partial\, \tau_{\kappa'\beta}} U^{\lambda}_{\kappa'\beta} = M_{\kappa}\omega^2_{\lambda} U^{\lambda}_{\kappa\alpha}, \tag{3}$$

with eigenfrequencies ω and eigendisplacements $\mathbf{U}$ pertaining to mode λ (here V is the potential energy and M the ionic masses). The $\mathbf{U}$'s are normalized according to

$$\sum_{\kappa\alpha} M_{\kappa} U^{\lambda^2}_{\kappa\alpha} = 1. \tag{4}$$

The dipole $\mathbf{Z}^{\lambda}$ obtained from Eq. (2) for the eigenmode U^{λ} is usually called the charge vector of the mode. Modes with a finite charge vectors are called transverse-optical (TO) modes because they are involved in radiative transitions. The matrix elements for such transitions are proportional to charge vectors, which are thus directly accessible through infrared spectroscopy.[8]

The lattice dielectric constant is decomposed in contribution coming from each TO mode.[9] In terms of the mode charge vectors this sum is written as

$$\epsilon^{\alpha\beta}_{lat} = \frac{4\pi}{\Omega} \cdot \sum_{\lambda} \frac{Z^{\lambda}_{\alpha} \cdot Z^{\lambda}_{\beta}}{\omega^2_{\lambda}}. \tag{5}$$

To evaluate the dielectric constants, we need dynamical Born charges, the electronic part ϵ_{∞} of the dielectric constant, and the eigensystem of the $\mathbf{k}=0$ dynamical matrix. Dynamical Born charges and ϵ_{∞} are calculated using the density-functional perturbative approach.[11–13] The zone-center dynamical matrix is obtained from centered-difference derivatives of the forces on each ion with respect to displacements of ± 0.01 Å in each cartesian direction. All the present calculations employ the QUANTUM ESPRESSO (Ref. 14) package. The calculations further use a plane-wave basis (cutoff 35 Ryd), Vanderbilt ultrasoft pseudopotentials,[15] and the generalized gradient approximation[16] for exchange and correlation.

III. RESULTS

The body-centered cubic unit cell of bixbyite includes 40 atoms and has the $Ia\bar{3}$ space symmetry group. The group is constituted by 24 space operations, that include the inversion and all the rotations by π around (100) axes, and by $2\pi/3$ around (111) axes.[17] Besides the cubic lattice constant, there are four internal cell parameters named x, u, v, and w. Four of the cations are placed at 8b Wyckoff positions generated by cycling the group operations to the starting (1/4,1/4,1/4) position; the 12 remaining cations occupy the 24d position set, which encloses all the $(x,0,1/4)$ symmetric equivalents. The 24 oxygens occupy the 48e Wyckoff set generated by a (u,v,w) starting point. Table I reports the calculated structural parameters for the Sc, La, and Dy oxides. The internal parameter are quite similar; as they are expressed in units of the lattice constant, this means that the structure simply scales with the M-O bond length.

TABLE I. Structural parameters of the studied bixbyites. The internal parameters are in units of the lattice constant a_0.

	a_0 (Å)	x	(u,v,w)
Sc_2O_3	9.94	−0.036	(0.391,0.154,0.381)
Dy_2O_3	10.95	−0.034	(0.391,0.152,0.380)
La_2O_3	11.32	−0.028	(0.390,0.148,0.377)

The Born dynamical charge tensors of the 8b cations has three independent components, one for the diagonal component and two off-diagonal. The off-diagonal components change matrix location and sign depending on the site, their average vanishes as required by the cubic symmetry of the system. In Sc_2O_3 the diagonal is 3.89 and the off-diagonal are (0.45, 0.57); in Dy_2O_3 the values are 3.8 and (0.45, 0.5); in La_2O_3 they are 3.97 and (0.49, 0.49).

The 24d cation charge tensor has five independent components (three on the diagonal plus two off-diagonal terms) which change sign and position each site; four of the off-diagonal terms are identically vanishing by symmetry. The Sc_2O_3 diagonal terms are (3.55, 4.04, 3, 61) and the off-diagonal are (0.51, 0.38). The Dy_2O_3 values are (3.4, 3.9, 3.5) and (0.43, 0.37); those for La_2O_3 are (3.53, 3, 95, 3, 66) and (0.36, 0.37).

The 48d charge tensor of oxygens has nine independent components. For Sc_2O_3 the diagonal terms are (−2.34, −2.4, −2.81) and the off-diagonal terms average in absolute value to 0.19. For Dy_2O_3 the diagonal terms are (−2.3, −2.4, −2.8) and the average off-diagonal term is 0.16. In La_2O_3 we have (−2.43,−2.52,−2.85) and an off-diagonal average of 0.17. In all cases the effective charges are anomalous, i.e., sizably larger than the nominal ionic charge (though not as much as in, e.g., titanates). The acoustic sum rule, stating dynamical charge neutrality, is verified computationally to within 0.1 electron charges (or about 2%) on the diagonal components.

The electronic contribution to the static dielectric constant ϵ_{∞} in bixbyites reduces to a simple scalar because of cubic symmetry. The computed ε_{∞} for Sc_2O_3, Dy_2O_3, and La_2O_3 are similar and fairly small: 4.6, 4.1, and 4.2, respectively.

The space of periodic displacements on bixbyites has the irreducible representation decomposition[17]

$$\Gamma_{disp} = 4A_g \otimes 5A_u \otimes 4E^1_g \otimes 5E^1_u \otimes 4E^2_g \otimes 17T_u \otimes 14T_g.$$

By symmetry, only modes belonging to three-dimensional T_u representations can develop a nonvanishing dipole. For the

TABLE II. Energies (cm^{-1}) and logarithm of oscillator strengths (cm^{-2}) for polar modes in bixbyites.

Sc_2O_3		Dy_2O_3		La_2O_3	
ω	log(S)	ω	log(S)	ω	log(S)
166	2.52	83	2.15	80	2.62
198	3.46	106	1.40	101	2.60
217	3.73	116	2.65	110	2.44
233	4.62	123	3.35	117	3.71
251	2.77	135	2.49	130	3.70
285	4.99	170	2.78	160	2.89
297	5.02	207	2.15	203	5.25
326	5.73	267	5.54	208	4.70
344	5.30	295	4.78	217	5.25
361	3.96	309	4.93	232	4.53
374	5.64	330	4.05	251	5.43
421	2.97	340	5.36	257	4.61
443	3.73	384	4.20	303	4.15
470	3.65	432	3.96	315	3.36
506	4.00	458	3.51	335	3.21
589	4.56	520	4.47	462	3.83

rigid-translations set T_u triplet, the dipole vanishes by the acoustic sum rule. Each of the remaining 16 triplets develop dipoles in mutually orthogonal directions, as required by the electric isotropy of the cubic system. Table II reports the frequency and the oscillator strength of the T_u modes. Oscillator strengths are the squared dipole of the mode times $4\pi/\Omega$ and in atomic units have the dimension of a squared energy. We use the same units as for mode energies.

In Fig. 1 we compare the moduli of the total dipoles and their partial component generated by the oxygen displacements. Oxygen and cation partial dipoles have to be either parallel or antiparallel; all modes with significantly large dipoles present parallel partial dipoles. One can observe that oxygens generate always the most part of the dipoles, analogously to what already reported for Lu_2O_3.

The contributions of each polar mode to the static dielectric constant is given by its oscillator strength divided by its squared frequency. For Sc_2O_3 we have a total lattice contribution of 13.4 which added to the electronic part yields a total static dielectric constant of 18. For Dy_2O_3 the lattice contribution is equal to 9.0 and the total static dielectric constant is equal to 13.1. For cubic La_2O_3 we obtain a lattice contribution of 15.9 and a total ε of 20. The values are summarized in Table III. In Fig. 2 we show the frequency-dependent dielectric intensity, i.e., the partial contributions of each polar mode to the static dielectric constant of the three materials. The data in this figure can be compared with those for Lu_2O_3, curve (b) in Fig. 1 of Ref. 8. A strong similarity in shape and peak spacing is evident between Dy_2O_3 and Lu_2O_3, except that the latter has a spectrum shifted to higher energies. This accounts for the small difference in the ionic dielectric constants (see Table III).

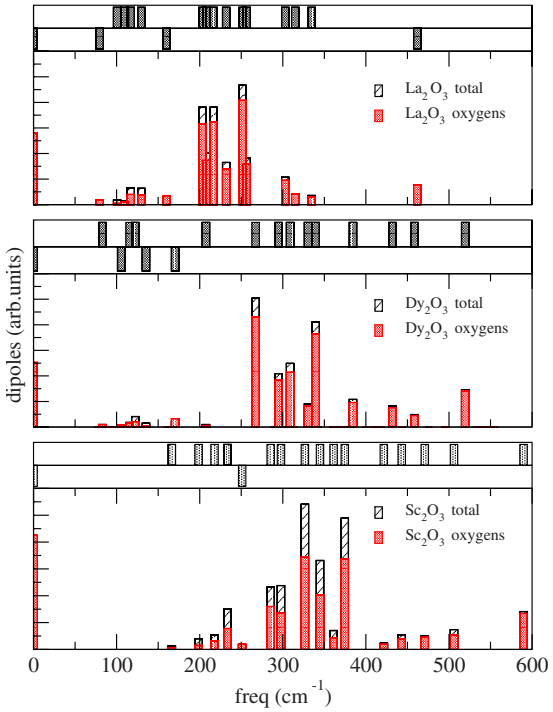

FIG. 1. (Color online) Mode charge vectors moduli and their partial oxygen component. For each oxide in the top panel we show the cosine of the angle between oxygen component and cation component; only possible cosines are ± 1.

IV. DISCUSSION

To analyze the different character of the IR active vibrational modes, Fig. 3 reports as a function of mode energy our measure of the localization of a mode (i.e., a collective displacement), namely, $M_\kappa|\mathbf{u}_\kappa|^2$ with $\mathbf{u}_\kappa$ the displacement amplitude of the κth ion [since the eigendisplacements are normalized according to Eq. (4), the sum of all localizations of each mode is unity; acoustic modes at zero energy have a larger localization on cations due to their larger mass]. For rare-earth oxides, where the cation and oxygen masses differ by 1 order of magnitude, the calculations clearly bear out a sharp separation between low-energy modes (prevailingly consisting of cation displacements) and higher-frequency modes (where oxygen motions prevail). The transition between the two groups is around 200 cm^{-1}, for both Dy and La oxides, as well as Lu_2O_3.[8] In La_2O_3 the oxygen-modes range actually starts immediately at the end of the cation-mode range while in dysprosium oxide there is a gap of

TABLE III. Dielectric constants of bixbyites. Previously calculated data for lutetia are included for comparison.

	ε_∞	$\varepsilon_{\text{ionic}}$	ε
Sc_2O_3	4.6	13.4	18.0
La_2O_3	4.1	15.9	20.0
Dy_2O_3	4.1	9.0	13.1
Lu_2O_3 [a]	4.2	7.8	12.0

[a]Reference 8.

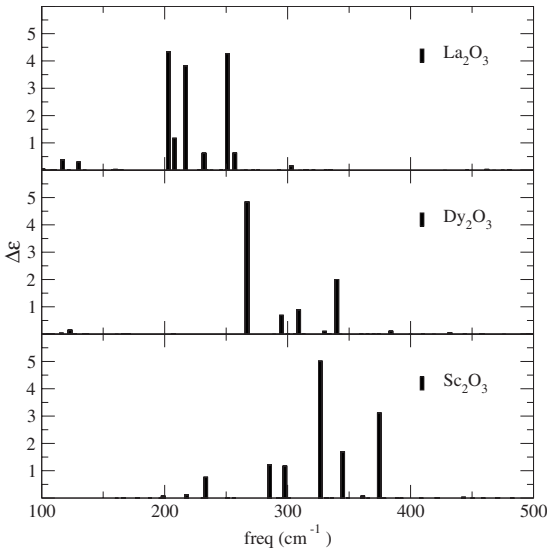

FIG. 2. Computed dielectric intensity (i.e., partial contributions to lattice part of the dielectric constant from polar modes) vs energy.

about 50 cm^{-1} between the two groups. This difference is probably caused by the much softer bonding in the first case. The oxygen modes of Dy_2O_3 being shifted up, the ionic contribution to the dielectric constant is sizably smaller than in La_2O_3 (Table III). As mentioned, a similar behavior in the mode character can be observed (though it was not made explicit in the original paper) in Lu_2O_3.[8]

At variance with the two rare-earth oxides, a character mixing between cation and anion displacements shows up in Sc_2O_3, where the cation/anion mass ratio is lower by a factor of over 3. We can single out a low-frequency cation-modes group up to 250 cm^{-1}, a high-frequency oxygen-modes group upward of 450 cm^{-1}, and a midrange (280–400 cm^{-1}) group containing modes of both kinds as well having mixed character. In mixed modes, the localization on cations decreases steadily with frequency (except in a few genuinely

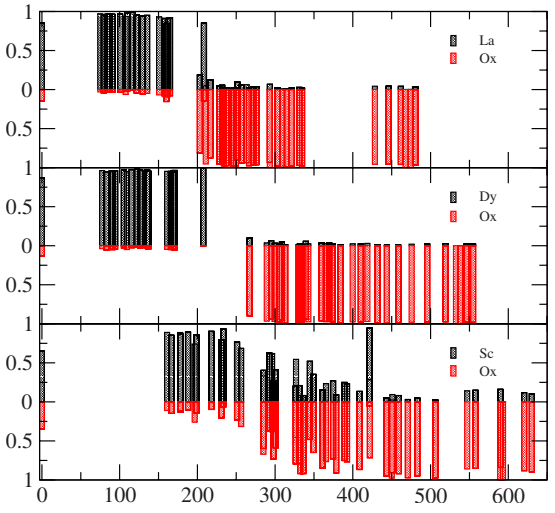

FIG. 3. (Color online) Localization of vibrational mode on cations and oxygens.

cationic modes such as the one at 421 cm^{-1}), but mixing does still cause some cationic modes to develop appreciable dipoles. This actually happens also for one La_2O_3 cationic mode at 207 cm^{-1}, bordering the oxygen range: comparing Figs. 1 and 3 one notices that the mode has prevailing cationic localization but the dipole is generated by oxygen displacements. The analogous mode in dysprosium oxide, at the border of the spectral gap, has instead no oxygen localization at all, and its dipole is very small. Also, because of the "gap closure" in La_2O_3 we find that five modes contribute importantly to the dielectric constant, whereas they are only four in Dy_2O_3, as in lutetia. Also because of this feature, the lattice dielectric constant in cubic lanthanum oxide is significantly larger than in dysprosia, even though the dipoles in the latter are actually larger.

In Sc_2O_3 the mixing affects all the modes relevant for the lattice screening. Looking at Fig. 1, the contribution of Sc displacements to dipoles is appreciable for all mixed modes. (Similar cation contributions to dipoles at these energies has been previously reported[18] in amorphous Sc_2O_3.) As mixing enhances dipoles, at lower frequencies we now find at least six modes giving a sizable contributions to the lattice dielectric constant.

V. CONCLUSIONS

Analyzing the data for different bixbyites, a clear dependence on cation mass and ionic radius emerges. Large dipoles are always due to oxygen displacements. Low-frequency modes have small oxygen motion components but the localization on oxygen increases with frequency. (Therefore, significant contributions to ε_{latt} come from midrange frequencies.) The frequency of cation-localized modes depend weakly on the cation; oxygen-localized modes instead shift down in energy as the ionic radius increases. In the extreme case of La, the two types of modes have overlapping frequency ranges. This produces an enhancement of the La_2O_3 dielectric constant, both because of the downshift and because a cationic-mode dipole is increased by the mixing with oxygen displacement modes.

Sc has a much shorter radius than rare earths and is a factor 3–4 less massive. In scandia, in fact, cationic modes range up to 420 cm^{-1}. Because of the stiffer bonds, oxygens modes begin at still higher frequencies than in the other compounds. Modes in the intermediate range have mixed character. Cations displacements contribute sizably to the total dipole, also because of the lighter cation. Although the most intense dielectric modes have higher frequencies, in Sc_2O_3 the dielectric constant is larger than in Dy and Lu oxides, and not far from La oxide, because more contributions are present.

In summary, the present calculations provide a rationale for the trends of dielectric screening in bixbyite sesquioxides. The conclusion apropos technological interest is that cubic sesquioxides are expected not to escape, roughly, the 12–18 value range of dielectric constants, and therefore are not especially strong candidate high-ε materials, all the more so in the perspective of smaller-size technology nodes requiring ultrahigh (50 and above) ε's.

ACKNOWLEDGMENTS

Work supported in part by the Italian Ministry of University and Research through project PON-Cybersar, by Fondazione Banco di Sardegna, by CASPUR Rome through a collaborative agreement, by CINECA through supercomputing grants, and by the EU within projects ATHENA and OxIDes.

[1] P. S. Peercy, Nature (London) **406**, 1023 (2000).
[2] G. D. Wilk, R. M. Wallace, and J. M. Anthony, J. Appl. Phys. **89**, 5243 (2001).
[3] G. Lucovsky, in *The 47th International Symposium: Vacuum, Thin Films, Surfaces/Interfaces, and Processing* (AVS, Boston, 2001), Vol. 19, p. 1553.
[4] L. Marsella and V. Fiorentini, Phys. Rev. B **69**, 172103 (2004).
[5] D. Schlom and J. Haeni, MRS Bull. **27**, 198, (2002).
[6] P. Delugas, V. Fiorentini, A. Filippetti, and G. Pourtois, Phys. Rev. B **76**, 104112 (2007).
[7] P. Delugas and V. Fiorentini, Microelectron. Reliab. **45**, 831 (2005); R. Lo Nigro, R. G. Toro, G. Malandrino, V. Raineri, and I. L. Fragalà, Adv. Mater. (Weinheim, Ger.) **15**, 1071 (2003); P. Delugas, V. Fiorentini, and A. Filippetti, in *Rare Earth Oxide Thin Films: Growth, Characterization, and Applications*, Topics Appl. Phys. Vol. 106, edited by M. Fanciulli and G. Scarel (Springer, Berlin, 2006), p. 225; V. Fiorentini, P. Delugas, and A. Filippetti, in *Advanced Gate Stacks for High-Mobility Semiconductors*, Series in Advanced Microelectronics Vol. 27, edited by A. Dimoulas, E. Gusev, P. C. McIntyre, and M. Heyns (Springer, Berlin, 2007), p. 269.
[8] E. Bonera, G. Scarel, M. Fanciulli, P. Delugas, and V. Fiorentini, Phys. Rev. Lett. **94**, 027602 (2005).
[9] M. Born and K. Huang, *Dynamical Theory of Crystal Lattices* (Oxford University Press, Oxford, 1954).
[10] W. Cochran and R. A. Cowley, J. Phys. Chem. Solids **23**, 447 (1962).
[11] S. Baroni, S. de Gironcoli, A. Dal Corso, and P. Giannozzi, Rev. Mod. Phys. **73**, 515 (2001).
[12] X. Gonze and C. Lee, Phys. Rev. B **55**, 10355 (1997).
[13] S. Baroni, P. Giannozzi, and A. Testa, Phys. Rev. Lett. **58**, 1861 (1987).
[14] P. Giannozzi, S. Baroni, N. Bonini, M. Calandra, R. Car, C. Cavazzoni, D. Ceresoli, G. L. Chiarotti, M. Cococcioni, I. Dabo, A. Dal Corso, S. Fabris, G. Fratesi, S. de Gironcoli, R. Gebauer, U. Gerstmann, C. Gougoussis, A. Kokalj, M. Lazzeri, L. Martin-Samos, N. Marzari, F. Mauri, R. Mazzarello, S. Paolini, A. Pasquarello, L. Paulatto, C. Sbraccia, S. Scandolo, G. Sclauzero, A. P. Seitsonen, A. Smogunov, P. Umari, and R. M. Wentzcovitch, J. Phys.: Condens. Matter **21**, 395502 (2009).
[15] D. Vanderbilt, Phys. Rev. B **41**, 7892 (1990).
[16] J. P. Perdew, J. A. Chevary, S. H. Vosko, K. A. Jackson, M. R. Pederson, D. J. Singh, and C. Fiolhais, Phys. Rev. B **46**, 6671 (1992).
[17] M. I. Aroyo, A. Kirov, C. Capillas, J. M. Perez Mato, and H. Wondratschek, Acta Crystallogr. A **62**, 115 (2006); M. I. Aroyo, J. M. Perez Mato, C. Capillas, E. Kroumova, S. Ivantchev, G. Madariaga, A. Kirov, and H. Wondratschek, Bilbao crystallographic server: I. databases and crystallographic computing programs, 2005, http://www.atypon-link.com/OLD/doi/abs/10.1524/zkri.2006.221.1.15
[18] P. Delugas, V. Fiorentini, and A. Filippetti, Appl. Phys. Lett. **92**, 172903 (2008).
[19] X.-Q. Chen, C. L. Fu, C. Franchini, and R. Podloucky, Phys. Rev. B **80**, 094527 (2009).